Published OnlineFirst July 28, 2017; DOI: 10.1158/1078-0432.CCR-16-2598

Biology of Human Tumors

Clinical Cancer Research

Tumor Purity as an Underlying Key Factor in Glioma

Chuanbao Zhang[1], Wen Cheng[2], Xiufang Ren[3], Zheng Wang[1], Xing Liu[1], Guanzhang Li[1], Sheng Han[2], Tao Jiang[1], and Anhua Wu[2]

Abstract

Purpose: Glioma tissues consist of not only glioma cells but also glioma-associated nontumor cells, such as stromal cells and immune cells. These nontumor cells dilute the purity of glioma cells and play important roles in glioma biology. Currently, the implications of variation in glioma purity are not sufficiently clarified.

Experimental Design: Here, tumor purity was inferred for 2,249 gliomas and 29 normal brain tissues from 5 cohorts. Based on the transcriptomic profiling method, we classified CGGA and TCGA-RNAseq cohorts as the RNAseq set for discovery. Cases from TCGA-microarray, REMBRANDT, and GSE16011 cohorts were grouped as a microarray set for validation. Tissues from the CGGA cohort were reviewed for histopathologic validation.

Results: We found that glioma purity was highly associated with major clinical and molecular features. Low purity cases were more likely to be diagnosed as malignant entities and independently correlated with reduced survival time. Integrating glioma purity into prognostic nomogram significantly improved the predictive validity. Moreover, most recognized prognostic indicators were no longer significantly effective under different purity conditions. These results highlighted the clinical importance of glioma purity. Further analyses found distinct genomic patterns associated with glioma purity. Low purity cases were distinguished by enhanced immune phenotypes. Macrophages, microglia, and neutrophils were mutually associated and enriched in low purity gliomas, whereas only macrophages and neutrophils served as robust indicators for poor prognosis.

Conclusions: Glioma purity and relevant nontumor cells within microenvironment confer important clinical, genomic, and biological implications, which should be fully valued for precise classification and clinical prediction. *Clin Cancer Res; 23(20); 6279–91. ©2017 AACR.*

Introduction

Glioma is the most common and lethal type of tumor in the central nervous system (CNS). Traditional histopathology classifies gliomas chiefly based on glioma cell features, including microscopic similarities with putative origin cells and presumed levels of differentiation. Emerging molecular advances integrate the genotype of glioma cells, including IDH mutation and the 1p/19q codeletion, into the 2016 CNS World Health Organization (WHO) classification (1). Even though increasing studies uncover mechanisms affecting the malignant properties of glioma cells and identify reasonable therapeutic targets (2, 3), the current clinical prediction and treatment outcome are still not satisfactory.

At present, we are deeply aware that glioma tissues contain abundant glioma-associated nontumor cells within their microenvironment. These nontumor cells play important roles in glioma development and are represented by stromal and immune cells (4, 5). Studies reveal that stromal cells are deeply involved in glioma proliferation, invasion, and angiogenesis (6–9). Furthermore, increasing evidence indicates that infiltrating immune cells have diverse roles in glioma biology (10, 11). Indeed, even nontumor cells dilute the purity of glioma cells. They mutually cooperate to maintain a subtle homeostasis for gliomagenesis, malignancy progression, and treatment resistance (12). However, current classification systems apply little attention to the nontumor fractions within glioma tissue, and there is limited knowledge on the characteristics of glioma cells under various purities.

A proper analytical model is necessary for exploring this issue. Recently, Yoshihara and colleagues have developed a universal algorithm based on transcriptomic expression data to infer tumor purity—quantifying tumor cell content in the tissue—and estimate infiltration of stromal and immune cells (13). Here, transcriptomic data of 2,249 gliomas and 29 normal brain tissues were collected for analysis. Tumor purity was calculated using the ESTIMATE algorithm (13). The role of glioma purity was systematically investigated in clinical, genomic, and biological conditions, which may provide novel insights into the glioma microenvironment and aid in the development of robust classification and predictive systems.

[1]Beijing Neurosurgical Institute, Capital Medical University, Beijing, China. [2]Department of Neurosurgery, The First Hospital of China Medical University, Shenyang, China. [3]Department of Pathology, Shengjing Hospital of China Medical University, Shenyang, China.

Note: Supplementary data for this article are available at Clinical Cancer Research Online (http://clincancerres.aacrjournals.org/).

C. Zhang and W. Cheng contributed equally to this article.

Corresponding Authors: Anhua Wu, The First Hospital of China Medical University, Nanjing Street 155, Heping District, Shenyang, Liaoning 110001, China. Phone: 8602483283301; Fax: 8602483283301; E-mail: wuanhua@yahoo.com; or Tao Jiang, Beijing Neurosurgical Institute, Capital Medical University, No.6 Tiantan Xili, Dongcheng District, Beijing 100050, China. Phone: 861067021832; Fax: 861067096713; E-mail: taojiang1964@163.com

doi: 10.1158/1078-0432.CCR-16-2598

Published OnlineFirst July 28, 2017; DOI: 10.1158/1078-0432.CCR-16-2598

Translational Relevance

Glioma tissues are always intermixed with a considerable fraction of nontumor cells. Whereas, current classification and prediction systems apply little attention to the purity of glioma cells. Here, we found that glioma purity correlated with several clinical features. Low purity cases were more likely to be diagnosed as malignant entities and lead to a poor prognosis. Different glioma purity also indicated diverse genomic aberrations and biological phenotypes. Low purity gliomas were characterized by intensive local immune phenotypes and enriched with macrophages, neutrophils, and microglia. Whereas, only macrophages and neutrophils served as robust indicators for poor prognosis. This research offers a comprehensive evaluation of the importance of glioma purity in multidimensional conditions and identifies the resulting enriched immune cells. These findings may facilitate the full understanding of microenvironmental biology and offer novel insights into glioma classification, prognostic prediction, and effective therapeutic strategy.

Materials and Methods

Patients

This study collected 2,249 gliomas and 29 normal brain tissues from four databases: CGGA (China), TCGA (the United States), REMBRANDT (the United States), and GSE16011 (the Netherlands). There are two available cohorts of gliomas in the TCGA database. Accordingly, five glioma cohorts were involved in this study: CGGA, TCGA-RNAseq, TCGA-microarray, REMBRANDT, and GSE16011. Based on the transcriptomic profiling method, we grouped CGGA and TCGA-RNAseq cohorts into an RNAseq set for discovery. Whereas, cases from TCGA-microarray, REMBRANDT, and GSE16011 cohorts were classified into a microarray set for validation.

The CGGA cohort consisted of 325 cases whose clinical and molecular information was obtained from the CGGA database (http://www.cgga.org.cn). Each case enrolled was treated by members of the CGGA group. Tumor tissue samples were collected at the time of surgery after informed consent. Neuropathologists established the diagnosis and ensured the quality of the tissue for molecular testing (14). Overall survival (OS) was calculated from the date of diagnosis until death or the end of follow-up. The point of death is defined by death certification, which could be obtained from local hospitals and police stations. Another 1,953 glioma cases were included from the TCGA (https://gdc.cancer.gov/), REMBRANDT (https://cainte grator.nci.nih.gov/rembrandt/), and GSE16011 (http://www.ncbi.nlm.nih.gov/geo/query/acc.cgi?acc=GSE16011) databases. Information on these patients is available from corresponding data portal. Patient characteristics are described in Supplementary Tables S1 and S2.

Ethical statement

Collection of tumor tissue and clinicopathologic information was undertaken with informed consent. Study protocols were approved by the ethics committees of the participating institutions. The study was conducted in accordance with the Declaration of Helsinki.

RNAseq and quality control

The libraries were sequenced on the Illumina HiSeq 2000 platform by the 101-bp pair-end sequencing strategy. Base calling (Illumina pipeline CASAVA v1.8.2) was used to convert original image data into sequence data. The sequence data were further processed to define improper reads according to standard quality control criteria. All reads that fit any of the following parameters were removed:

(1) The reads that aligned to adaptors or primers with no more than two mismatches.
(2) The reads with more than 10% unknown bases (N bases).
(3) The reads with more than 50% of low-quality bases (quality value ≤ 5) in one read.

Read mapping and expression analysis of RefSeq genes

We downloaded the Hg19 RefSeq (RNA sequences, GRCh37) from the UCSC Genome Browser (http://genome.ucsc.edu). The gene expression was estimated using the reads per kilobase transcriptome per million reads (RPKM) method (15). The RPKM method could remove the influence of different gene lengths and sequencing discrepancies from the expression calculation. Therefore, we could directly use the calculated gene expression data to compare the differences in gene expression among samples.

Evaluation of IDH mutation status by DNA pyrosequencing

Genomic DNA was extracted from frozen tissues using a QIAamp DNA Mini kit (Qiagen) according to the manufacturer's protocol. DNA concentration and quality were measured using a Nano-Drop ND-1000 spectrophotometer. Pyrosequencing of mutations in *IDH1* or *IDH2* was supported by Gene Tech and performed on a Pyro-Mark Q96 ID System (Qiagen). PCR amplification was performed using the primers 5′-GCT TGT GAG TGG ATG GGT AAA AC-3′, 5′-Biotin- TTG CCA ACA TGA CTT ACT TGA TC-3′ for *IDH1* and 5′-ATC CTG GGG GGG ACT GTC TT-3′, 5′-Biotin-CTC TCC ACC CTG GCC TAC CT-3′ for *IDH2*. Pyrosequencing was performed using the primers 5′-TGG ATG GGT AAA ACC T-3′ for *IDH1* and 5′-AGC CCA TCA CCA TTG-3′ for *IDH2* (16).

Evaluation of the TERT promoter mutation by Sanger sequencing

Mutational hotspots in the *TERT* core promoter were obtained [nucleotide numbers 1 295 228 (C228T) and 1 295 250 (C250T)] from the human reference sequence (GrCh37 February 2009; http://genome.ucsc.edu/). Nested PCR was used to amplify the mutational hotspots. The first PCR primer sequences were 5′-GTC CTG CCC CTT CAC CTT-3′ (forward) and 5′-GCA CCT CGC GGT AGT GG-3′ (reverse), which yielded a 273-bp product. Further nested PCR was conducted using primers (Primer set 2) 5′-CCG TCC TGC CCC TTC ACC-3′ (forward) and 5′-GGG CCG CGG AAA GGA AG-3′ (reverse), which yielded a 128-bp product. We purified products from the second PCR using Illustra ExoProStar (GE Healthcare). The purified products were subjected to direct sequencing on an ABI 3100 PRISM DNA sequencer with a Big-Dye Terminator cycle sequencing kit (Applied Biosystems). The quality of all PCR products was checked before sequencing using electrophoresis on 2% agarose gels (17).

Evaluation of MGMT promoter methylation by DNA pyrosequencing

Bisulfite modification of DNA was performed using an EpiTect kit (Qiagen). The *MGMT* promoter region was amplified using

Published OnlineFirst July 28, 2017; DOI: 10.1158/1078-0432.CCR-16-2598

primers as follows: 5′-GTT TYG GAT ATG TTG GGA TA-3′ and 5′-biotin-ACC CAA ACA CTC ACC AAA TC-3′. Gene Tech performed pyrosequencing analysis. We averaged the methylation values across seven CpG loci within the *MGMT* promoter. We defined methylation as samples with an average methylation value of >10%.

Hematoxylin and eosin staining and immunohistochemical staining

We reviewed 12 glioma tissues from the CGGA cohort to infer glioma purity through the visual evaluation of hematoxylin and eosin–stained slides. Results of morphologic purity were independently confirmed by two neuropathologists.

Paraffin-embedded tissues of 43 cases from the CGGA cohort were collected. Because there is no specific antibody to distinguish macrophage and microglia in the CNS, we selected antibody against Iba-1 (Abcam; ab5076, 1:1,000) to detect macrophage/microglia (5). Anti-neutrophil elastase (Abcam; ab68672, 1:1,000) was used to stain neutrophil. Immunohistochemistry of paraffin sections was performed as previously described (18). Briefly, the sections were incubated with primary antibody overnight at 4°C, and then incubated with respective secondary antibody (ZSGB, 1:200) at room temperature for 1 hour. After washing with PBS buffer, the sections were stained with DAB for 5 minutes, rinsed in water, and counterstained with hematoxylin. Quantitative evaluation was performed by examining each section using at least five different high-power fields (X40 objective and X10 eyepiece) with the most abundant stained cells. Stained cells were manually counted 3 times for each photograph independently by two investigators. The number of stained cells was determined by the average method.

Bioinformatic analysis

Stromal and immune scores were calculated using the ESTIMATE R package (https://sourceforge.net/projects/estimateproject/), and glioma purity was estimated according to the formula described in Yoshihara and colleagues (13). Based on the expression data, cases were classified into relevant subtypes using the TCGA and EM/PM (EM is the abbreviation for EGFR module; PM is the abbreviation for PDGFRA module) classification schemes (19, 20). We used GISTIC2.0 to assess copy-number alterations (CNA) associated with glioma purity. Locus with GISTIC value more than 1 or less than −1 was defined as an amplification or deletion, respectively. Knowledge on gene interactions and pathways was obtained from the KEGG website (http://www.kegg.jp/; ref. 21). The principal components analysis (PCA) package of R was used to profile transcriptomic patterns attributing to glioma purity. Significance analysis of microarrays (SAM) was used to identify differential genes based on the threshold of fold change more than 3 and FDR less than 0.05. Spearman correlation analysis was used to evaluate the association between gene expression and glioma purity. Gene sets were submitted to the DAVID website (http://david.abcc.ncifcrf.gov/home.jsp) to perform gene ontology (GO) analysis and to retrieve relevant biological implications (22). The biological phenotype was further verified using gene set enrichment analysis (GSEA; ref. 23). Associations between immune cells and glioma purity were analyzed using the gene set variation analysis (GSVA) package of R (24). The gene list of immune cells was summarized by Gabriela and colleagues (25) and Oleg and colleagues (26).

Statistical analysis

Associations between continuous variables were tested using Spearman correlation analysis. Differences in variables between groups were evaluated by the Student *t* test, one-way ANOVA, or Yate's continuity corrected χ^2 tests. The Kaplan–Meier survival curve was depicted to estimate survival distributions. The log-rank test was used to assess statistical significance between groups. Univariate cox and further backward stepwise multivariate cox regression analyses were performed to identify independent prognostic factors. A nomogram was formulated based on the results of multivariate cox regression analysis (27). The predictive validity was assessed by comparing nomogram-predicted with observed survival probability. Bootstraps with 1,000 resamples were applied to these activities. The performance of the nomogram was evaluated using the concordance index (C-index). A larger C-index indicated a more accurate prognostic prediction. Patients with missing information were excluded from corresponding analysis. All statistical analyses were conducted using R 3.3.0, SPSS software, and GraphPad Prism 6.0 software. A two-sided *P* value less than 0.05 was regarded as significant.

Results

Associations of glioma purity with clinical and molecular characteristics

A total of 2,249 gliomas and 29 normal brain tissues were included for analysis (Supplementary Tables S1 and S2). Four glioma cell lines (U87, U251, H4, and LN229 cell lines) were analyzed as references. We assessed glioma purity, as well as stromal and immune scores using the ESTIMATE algorithm. Morphology evaluation of glioma purity was conducted for 12 cases from the CGGA cohort (Supplementary Fig. S1A). Consistent with previous reports, glioma purity based on the ESTIMATE algorithm exhibited moderate correlation with morphology evaluation (Supplementary Fig. S1B and S1C; refs. 13, 28, 29). A high degree of purity was observed in glioma cell lines (median purity: 99.44%; Supplementary Table S3), verifying the validity of the ESTIMATE algorithm. There is a wide range of purity among the cases, 696 (30.95%) of the cases were highly purified (>90%), whereas 213 (9.47%) had poor purity (<60%; Supplementary Fig. S2B). In accordance with a previous report (13), we found a highly positive correlation between stromal and immune scores in glioma ($R = 0.9021$; Supplementary Fig. S2A).

Gliomas from the RNAseq and microarray sets were arranged in order of increasing purity (Fig. 1). The purity distribution was evaluated among groups and in association with other factors. We found a negative correlation between glioma purity and age at diagnosis (Fig. 1). Low purity gliomas were more likely to belong to mesenchymal and EM subtype. On the contrary, high purity gliomas were enriched in proneural and PM subtype (Supplementary Fig. S3A and S3E). With regard to genomic alterations, the IDH mutation and 1p/19q codeletion indicated higher glioma purity (Fig. 1; Supplementary Fig. S3). Even the TERT promoter mutation conferred lower purity in LGGs, and its influences were abolished in glioblastoma (GBM; Supplementary Fig. S3D). In addition, we also examined the correlation between purity and other parameters in stratified histopathology and molecular classification (Supplementary Table S4).

Published OnlineFirst July 28, 2017; DOI: 10.1158/1078-0432.CCR-16-2598

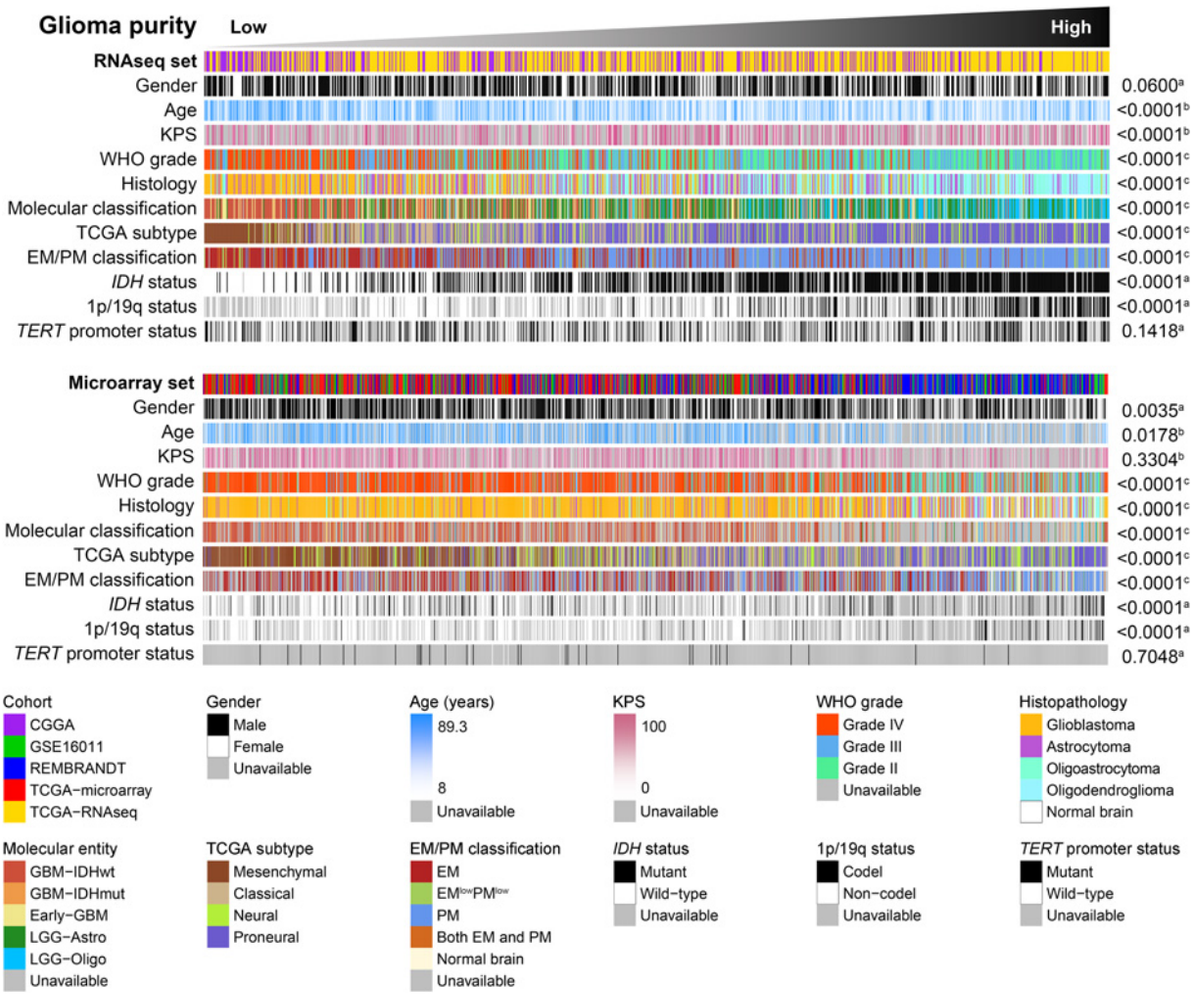

Figure 1.

Landscape of clinical and molecular characteristics in association with glioma purity. RNAseq (top) and microarray (bottom) sets were arranged in an increasing order of glioma purity. The relationship between glioma purity and patients' characteristics was evaluated (a, The distribution of glioma purity was assessed using the Student *t* test between two groups. b, The association between glioma purity and continuous variables was assessed using Spearman correlation tests. c, The distribution of glioma purity between several groups was assessed using one-way ANOVA).

Aggressive gliomas are characterized by higher stromal and immune scores, but lower purity

According to the WHO grading system and histogenetic features, gliomas were classified into corresponding entities. Stromal and immune scores significantly increased along with malignancy progression, whereas glioma purity decreased in higher grades (Fig. 2; Supplementary Table S3). With respect to histopathologic classification, oligodendroglioma had the lowest level of stromal and immune scores, but the highest purity. Contrarily, GBM was accompanied with high stromal and immune score, but low purity (Fig. 2; Supplementary Table S3).

Recent studies have incorporated important genetic alterations, such as *IDH* mutation, 1p/19q codeletion, and *TERT* promoter mutation, into glioma classification (30–32). Here, we divided gliomas into five molecular entities including lower-grade glioma (LGG)-Oligo (*IDH*-mutant LGG with *TERT* promoter mutation or 1p/19q codeletion), LGG-Astro (*IDH*-mutant LGG without *TERT* promoter mutation or 1p/19q codeletion), early-GBM (LGG with wild-type *IDH*), GBM-*IDH*mut (GBM with mutant *IDH*), and GBM-*IDH*wt (GBM with wild-type *IDH*). We found survival time was significantly reduced in an order of LGG-Oligo, LGG-Astro, Early-GBM, GBM-*IDH*mut, and GBM-*IDH*wt (Supplementary Fig. S4, $P < 0.0001$). In accordance with survival variation, stromal and immune scores were highest in GBM-*IDH*wt but lowest in LGG-Oligo (Fig. 2A–D; Supplementary Table S3). Glioma purity was highest in LGG-Oligo and lowest in GBM-*IDH*wt (Fig. 2E and F; Supplementary Table S3).

In addition, in RNAseq set, recurrent glioma or secondary GBM showed similar tumor purity as primary glioma (Supplementary Fig. S5A). When we focused on GBM, limited differences in tumor purity were observed among primary, recurrent, and secondary GBM (Supplementary Fig. S5B and S5C). These results indicated that recurrent glioma and secondary GBM had similar purity as primary cases.

Published OnlineFirst July 28, 2017; DOI: 10.1158/1078-0432.CCR-16-2598

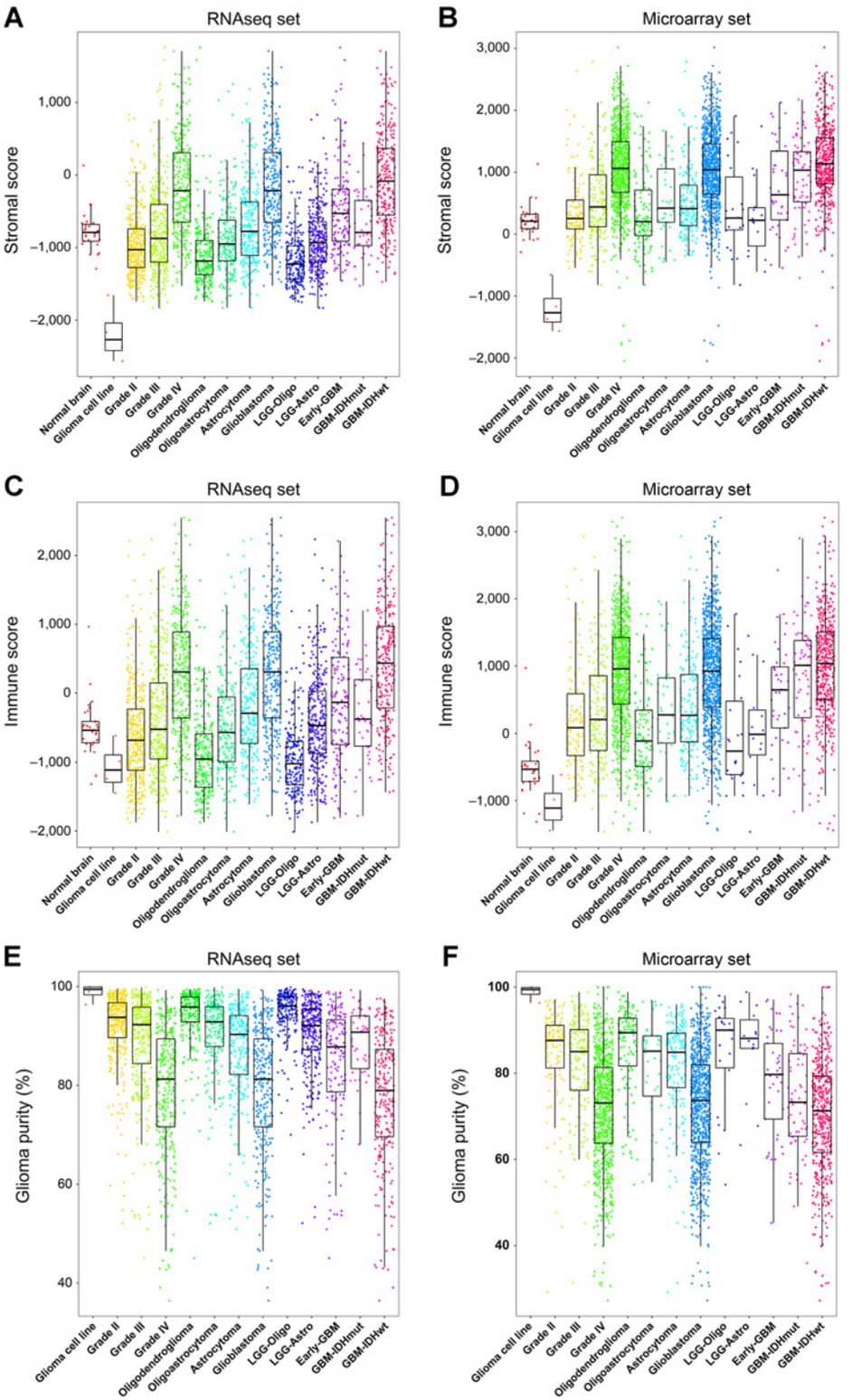

Figure 2.
Distinct distribution of stromal score, immune score, and tumor purity among glioma subtypes. Stromal score (**A** and **B**), immune score (**C** and **D**), and glioma purity (**E** and **F**) exhibited various distribution patterns among WHO grades, histopathologic classifications, and molecular entities.

Low glioma purity indicates unfavorable prognosis

We used the dichotomization on median value to separate cases for depicting the survival curves. Parallel analyses were conducted in both RNAseq and microarray sets. Cases with low purity generally had shorter OS than those with higher purity (Fig. 3A and B). Stratified analyses revealed that low purity conferred

Published OnlineFirst July 28, 2017; DOI: 10.1158/1078-0432.CCR-16-2598

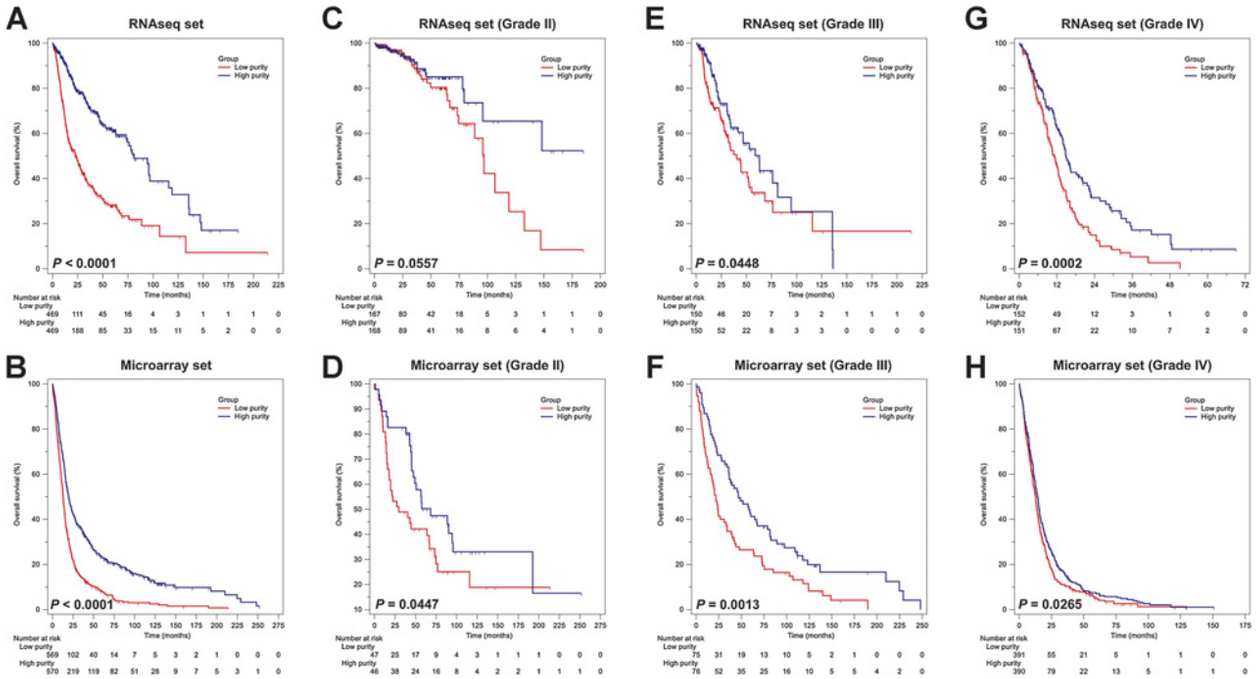

Figure 3.

Clinical outcome of different purity conditions. **A** and **B,** Different glioma purity conferred significantly different prognosis in all cases. **C–H,** The prognostic value of glioma purity in different grades.

reduced OS in most WHO grades except grade II in the RNAseq set (Fig. 3C–H). Survival curves were also depicted in different subtypes (Supplementary Fig. S6), recurrent gliomas, and secondary GBMs (Supplementary Fig. S7). Even though some of the tests failed to achieve statistical significance, low purity still implied a trend suggestive of inferior outcome in most subtypes and recurrent gliomas (Supplementary Figs. S6 and S7). In addition, similar analyses were applied for stromal (Supplementary Figs. S8 and S9) and immune scores (Supplementary Figs. S10 and S11), indicating that they were unfavorable indicators for prognosis.

We next conducted cox regression analyses to assess the prognostic independence of glioma purity among other factors. Glioma purity independently correlated with a better outcome in both RNAseq and microarray sets (Table 1). Among all cases, multivariate cox regression also confirmed that glioma purity along with age, Karnofsky performance score (KPS), radiation, chemotherapy, and 1p/19q status were independent prognostic indicators in glioma (Table 1). Afterward, these independent factors were integrated to develop a prognostic nomogram (Supplementary Fig. S12A). The calibration plot for the probability of survival at 1, 2, and 3 years showed an optimal agreement between the prediction by nomogram and actual observation (Supplementary Fig. S12B). We compared the predictive power for OS between nomograms and its constituting factors. The C-index for OS prediction was 0.736 (95% confidence interval, 0.656–0.816) by the nomogram, which was significantly higher than the C-indices of the constituting factors (Supplementary Fig. S12C). These results indicated that integrating glioma purity into a predictive model significantly improved the predictive validity.

Validity of recognized prognostic indicators in gliomas with divergent purity

Subsequently, the prognostic significance of known indicators was evaluated in gliomas with various purities. We sought to group all cases based on the median purity, but the sample size became limited owing to missing information and different proportion of cases among cohorts. Accordingly, we conducted the analyses in cases from the TCGA and CGGA databases, respectively. Cases were divided into low and high purity groups based on their median purity. Among traditional clinical and molecular factors, only KPS was verified as an independent prognostic factor for low purity gliomas in both TCGA and CGGA databases (Supplementary Table S5). In the high purity group, only histopathologic classification was identified with statistical significance. However, the improper HR, which was discrepant from the histopathology reality, undermined its validity (Supplementary Table S6). Accordingly, no factor could be deemed as an independent prognostic indicator for high purity gliomas in the present study. These results indicate the necessity of considering glioma purity for better prognostication.

Glioma purity associates with distinct patterns of genomic alterations

To uncover the molecular mechanisms influencing tumor cell percentage within glioma, TCGA cases with available mutation and CNA information were analyzed for that purpose. We found a negative correlation between somatic mutations and glioma purity ($R = -0.2434$, $P < 0.0001$; Supplementary Fig. S13A). Based on the increasing purity, cases were respectively divided into two, three, or four subgroups. Parallel analyses were conducted in each kind of grouping to enhance the credibility of our

Table 1. Univariate and multivariate cox analyses in gliomas

	RNAseq set					Microarray set					All cases				
		Univariate		Multivariate			Univariate		Multivariate			Univariate		Multivariate	
Factor	Number of samples	*P* value	HR	*P* value	HR	Number of samples	*P* value	HR	*P* value	HR	Number of samples	*P* value	HR	*P* value	HR
Age															
Increasing years	938	<0.0001	1.0578			779	<0.0001	1.0390	<0.0001	1.0259	1,717	<0.0001	1.0523	<0.0001	1.0306
Grade															
Malignancy progress	938	<0.0001	4.1653	0.0069	3.9990	1,024	<0.0001	2.1057			1,962	<0.0001	2.9327		
Histology	938	<0.0001		0.2446		1,124	<0.0001		0.0015			<0.0001			
Glioblastoma	303	Ref.	Ref.	Ref.	Ref.	858	Ref.	Ref.	Ref.	Ref.	1,161	Ref.	Ref.		
Astrocytoma	236	<0.0001	0.2040	0.0854	3.4748	132	<0.0001	0.3305	0.0664	0.4204	368	<0.0001	0.2698		
Oligoastrocytoma	187	<0.0001	0.1138	0.5535	1.6755	35	<0.0001	0.4140	0.9317	1.0519	222	<0.0001	0.1852		
Oligodendroglioma	212	<0.0001	0.0743	0.9674	<0.0001	100	<0.0001	0.3162	0.0003	0.3337	312	<0.0001	0.1737		
KPS															
Increasing score	454	<0.0001	0.9645	0.0002	0.9680	644	<0.0001	0.9774	<0.0001	0.9798	1,098	<0.0001	0.9711	0.0441	0.9876
Radiation															
Yes vs. No	287	<0.0001	0.4290	0.0056	0.4906	710	0.0002	0.4363	<0.0001	0.2215	997	0.0344	0.7627	0.0001	0.2395
Chemotherapy															
Yes vs. No	279	0.0795	1.3777			712	0.0001	0.7266	<0.0001	0.4363	991	0.0367	0.8539	<0.0001	0.4184
IDH status															
Mutation vs. Wild-type	931	<0.0001	0.1553			616	<0.0001	0.4528			1,547	0.0367	0.8539		
1p/19q status															
Codel vs. Noncodel	623	<0.0001	0.2451			651	<0.0001	0.2845	0.0148	0.5154	1,274	<0.0001	0.2577	0.0261	0.1961
TERT promoter status															
Mutation vs. Wild-type	561	0.4995	1.1029			37	0.0511	4.2860			598	0.0528	1.2987		
MGMT promoter status															
Methylated vs. Unmethylated	839	<0.0001	0.3679	0.0464	0.5961	476	0.5990	1.0887			1,315	<0.0001	0.3189		
Glioma purity															
Increasing percentage	938	<0.0001	0.0072	0.0052	0.0866	1,124	<0.0001	0.1317	0.0002	0.1889	2,063	<0.0001	0.0354	0.0004	0.1596

Published OnlineFirst July 28, 2017; DOI: 10.1158/1078-0432.CCR-16-2598

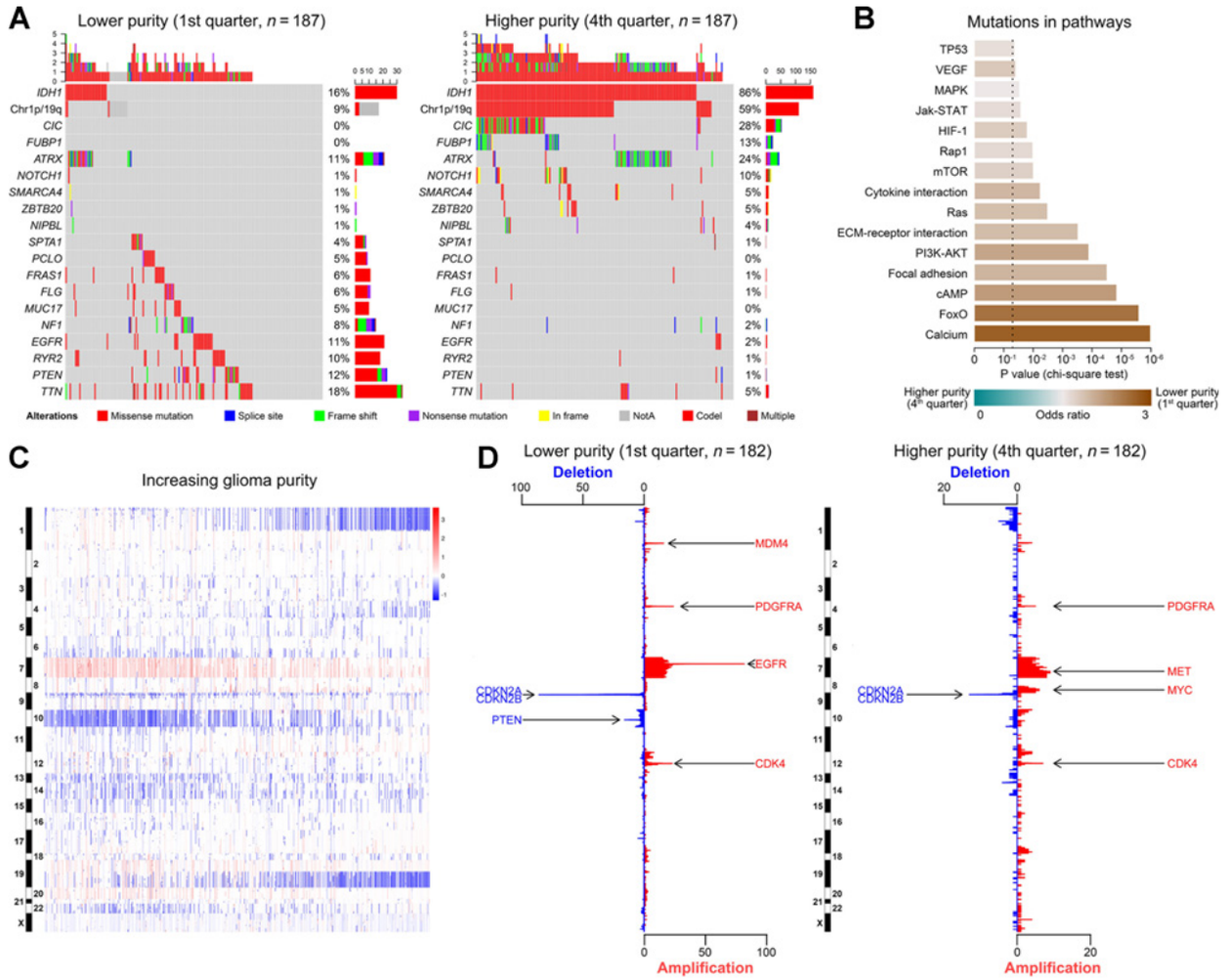

Figure 4.

Distinct genomic profiles associated with glioma purity. **A,** Differential somatic mutations were detected by comparing gliomas with low and high purity. **B**, Associations of mutations in pathways with glioma purity. The horizontal axis represents the significance of association, calculated using the χ^2 test. The dashed line corresponds to a *P* value of 0.05. **C,** The overall CNA profile in order of increasing glioma purity. **D,** A distinct CNA profile could be observed between gliomas with a low and high purity. The horizontal axis represents the frequency of chromosomal deletion (blue) and amplification (red).

findings. Here, we showed that the quartering condition was representative. First, we compared the frequency of mutations between cases with low and high purity. More somatic mutations were detected in cases with low purity (1st vs. 2nd half, 9,180 vs. 7,441 mutations; 1st vs. 3rd tertile, 6,532 vs. 4,790 mutations; 1st vs. 4th quarter, 4,872 vs. 3,518 mutations). Frequent mutations in IDH1, CIC, FUBP1, NOTCH1, as well as the 1p/19q codeletion were significantly enriched in cases with a higher purity (Fig. 4A; Supplementary Fig. S14A and S14B; Supplementary Table S7). On the other hand, mutations in *PTEN*, *EGFR*, and *NF1* occurred more frequently in gliomas with a lower purity (Fig. 4A; Supplementary Fig. S14A and S14B; Supplementary Table S7). We also observed that a significantly different frequency of mutations in *TTN*, *PCLO*, *MUC17*, *ZBTB20*, *NIPBL*, *FRAS1*, and *SPTA1* was attributed to various purity conditions, whereas existing studies have barely explored their roles in glioma.

Genomic mutations were further explored on the basis of KEGG pathways. Consistent with above findings, low purity cases carried more mutations in the 32 representative pathways (Supplementary Table S8). Calcium, FoxO, and cAMP pathways were the most significant differential pathways which had higher mutation rates among cases with low purity (Fig. 4B; Supplementary Fig. S14C and S14D; Supplementary Table S8). Meanwhile, a lower purity also indicated more mutations in genes involving focal adhesion, cell interaction, and recognized pathways in glioma, such as PI3K-AKT, Ras, and mTOR pathways (Fig. 4B; Supplementary Fig. S14C and S14D; Supplementary Table S8).

Subsequently, CNA data were investigated showing distinct chromosomal alteration patterns between gliomas with low and high purity. A negative correlation between CNAs and purity was found ($R = -0.2939$, $P < 0.0001$; Supplementary Fig. S13B). Consistently, more CNAs were detected in low purity gliomas

(1st vs. 2nd half, 81,515 vs. 52,961 CNAs; 1st vs. 3rd tertile, 54,944 vs. 31,362 CNAs; 1st vs. 4th quarter, 38,258 vs. 18,875 CNAs). The incidence of the 1p/19q codeletion, which is a genomic hallmark in oligodendroglioma, increased along with the increasing glioma cell percentage (Fig. 4C). Whereas, Chr 7 amplification paired with Chr 10 loss, a representative event in GBM (19), were enriched in low purity cases (Fig. 4C). A total of 808 genes were identified with a different frequency of amplification attributing to various glioma purities. Meanwhile, another 44 genes were differentially deleted in different purity situations (Supplementary Dataset S1). All these differential alterations occurred more frequently in the lower purity subgroups. Among cases with low purity, the frequently deleted genomic regions were 9p21.3 encompassing the *CDKN2A/CDKN2B* locus (47.25% in the 1st quarter; $P = 2.2E{-}17$) as well as 10q23.3 encompassing the *PTEN* locus (19.51% in the 1st quarter; $P = 0.0005$; Fig. 4D; Supplementary Fig. S14E and S14F). On the other hand, the most commonly amplified region associated with low purity was 7p11.2 encompassing the *EGFR* (45.05% in the 1st quarter, $P = 9.1E{-}24$; Fig. 4D; Supplementary Fig. S14E and S14F). *CDK4* (12q14.1; 12.64% in the 1st quarter; $P = 0.0043$) and *PDGFRA* (4q12; 13.19% in the 1st quarter; $P = 0.0005$) amplifications were also significantly frequent in low purity gliomas (Fig. 4D; Supplementary Fig. S14E and S14F).

Low purity glioma exhibits an intensive immune phenotype

Gene expression data were analyzed to explore the biological phenotypes associated with glioma purity. The TCGA-RNAseq cohort was selected as discovery set, and other cohorts were used for validation. We carried out PCA to explore the transcriptomic features associated with glioma purity. Here, we observed a tight association between whole transcriptome expression profile and glioma purity (Fig. 5A; Supplementary Fig. S15A–S15D), implying distinct general biological phenotypes attributing to various tumor cell percentage. Afterward, we sought to find out the biological features which are significantly enhanced in gliomas with low purity. We conducted spearman correlation analysis to identify genes associated with glioma purity. Genes whose expression were most negatively correlated with purity ($R < -0.8$) were submitted for GO analysis, showing that most of the top enriched biological implications were immune-relevant (Fig. 5B). Meanwhile, we divided cases into high and low purity groups based on the median purity. SAM was used to identify differential genes between cases with high and low purity. Genes that differentially upregulated in low purity cases were significantly enriched with terms related to immune response (Fig. 5C). Further, GSEA confirmed that cases with various glioma purity exhibited distinct immune status and low purity ones suffered a strengthened immune phenotype compared with high purity ones (Fig. 5D).

Macrophage and neutrophil are enriched in low purity glioma and indicate poor prognosis

As lower purity confers intensive local immune status, we sought to investigate which type of immune cell forms the nontumor fraction and contributes to the enhanced immune response. We employed GSVA for estimating signatures of multiple immune cells and correlated the signatures with glioma purity (Fig. 5E; Supplementary Fig. S15E–S15H). According to the association with glioma purity, immune cells could be clustered into two subgroups. A threshold of absolute correlation coefficient more than 0.3 was used for filtration across cohorts (Supplementary Table S9). Macrophages, neutrophils, and microglia exhibited consistent negative correlation ($R < -0.3$) with glioma purity. Whereas, central memory T cells, follicular helper T cells, CD8 T cells, natural killer (NK) cells, eosinophils, and T helper 1 cells were consistently positively correlated ($R > 0.3$) with glioma purity. A mutual relationship clustered these immune cells into two subgroups (Fig. 5F; Supplementary Fig. S15I–S15L), which were in accordance with their correlation to glioma purity. We further collected 43 tissues from the CGGA cohort. IHC analysis confirmed that numbers of macrophage/microglia and neutrophil were enriched in low purity cases (Fig. 5G and H) and diversely correlated with glioma purity (Supplementary Fig. S16). Therefore, macrophages, microglia, and neutrophils could be a cluster of immune cells that contributed to the nontumor fraction within low purity gliomas. Considering macrophages, neutrophils, and microglia were highly enriched in gliomas with fewer tumor cells, we attempted to investigate their prognostic implications. Survival analyses showed macrophages and neutrophils, but not microglia, were significantly correlated with glioma prognosis (Fig. 5I–K). Similar analyses in other cohorts confirmed that enrichment of macrophages and neutrophils indicated reduced survival time (Supplementary Fig. S17).

Discussion

Tumor tissues have a diverse mixture of tumor and nontumor cells within their microenvironments. Tumor purity is routinely determined by pathologists through visual evaluation, which could be affected by the sensitivity of histopathology, interobserver bias, and variability in accuracy (33). Other than routine pathology-based estimation, genomic advances introduce many computational methods to determine tumor purity based on multiform genomic data, such as somatic mutation (34), somatic CNA (29), and DNA methylation (35), which elicit objective and highly concordant results (28). Owing to the compatibility of ESTIMATE algorithm in both microarray- and RNAseq-based transcriptome profiles, we reviewed 2,249 glioma cases and systematically investigated the role of glioma purity in present study. Glioma purity was highly associated with major clinical and genomic features, strengthening that glioma purity is an intrinsic characteristic of the tumor cell in developing a suitable microenvironment (28).

We found cases with low purity glioma cells exhibited few favorable implications but were more likely to be ascribed in malignant entities and have reduced survival time. On the one side, glioma cells with limited proliferative and invasive properties tend to grow slowly and form a solid bulk with less nontumor cell infiltration. On the other side, tumor cells have been reported to be capable of dominating a microenvironment (11), giving rise to the hypothesis that malignant gliomas recruit abundant surrounding cells and subjugate them to compose a protective shield. Therefore, low tumor purity and correlated cellular heterogeneity are responsible for glioma's aggressive phenotype and poor prognosis. Purity of glioma cells may add a new dimension in estimating malignant identities and explain why most therapeutic strategies aimed purely against glioma cells do not have an ideal outcome.

Glioma purity was identified as a robust indicator for prognosis, whereas most prognostic indicators were no longer

Published OnlineFirst July 28, 2017; DOI: 10.1158/1078-0432.CCR-16-2598

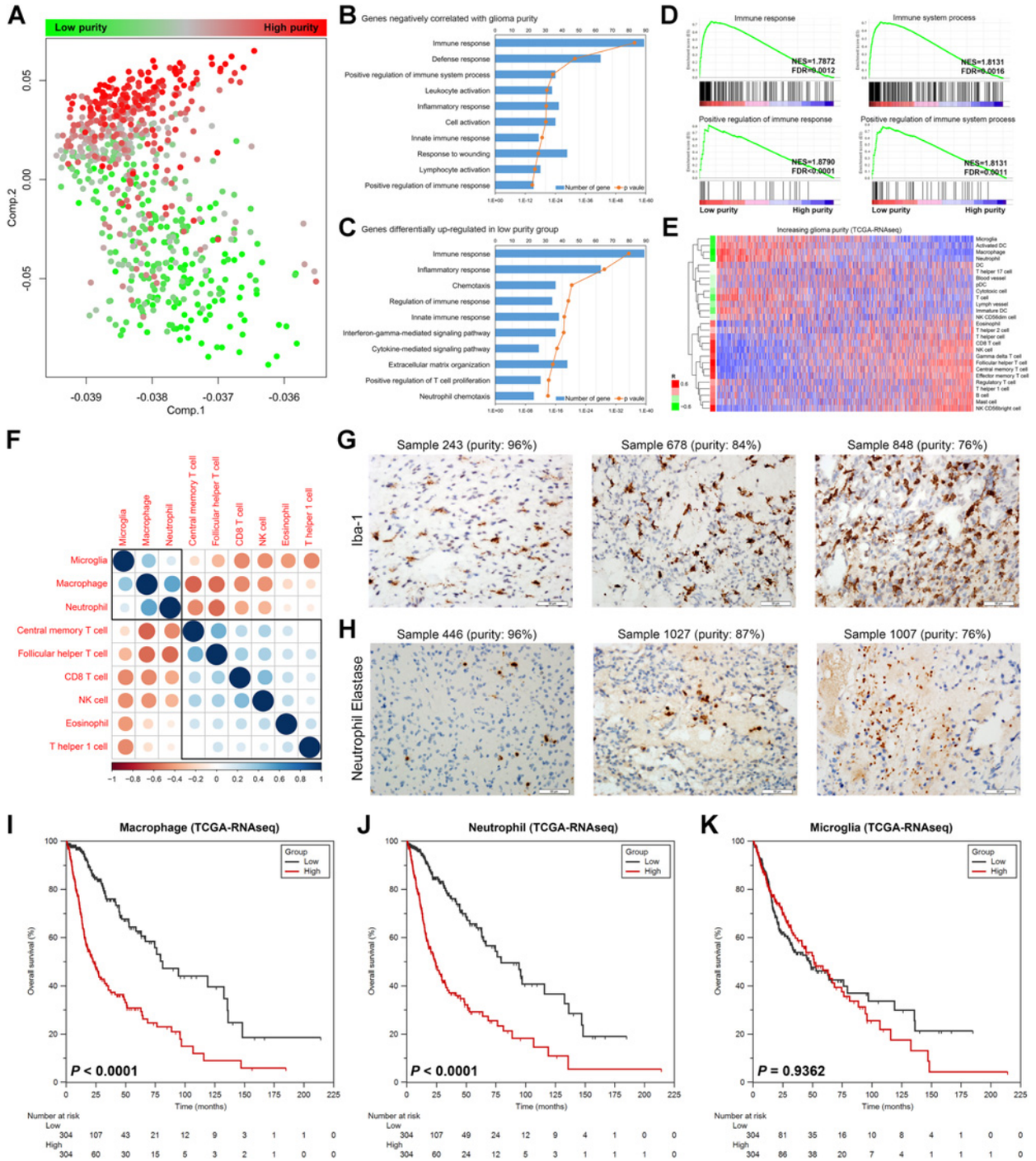

Figure 5.

Low purity glioma was characterized by an enhanced local immune response. **A,** There is a tight correlation between glioma purity and transcriptomic expression profiles. **B,** Immune relevant processes were the main biological implication originating from genes that were negatively correlated with glioma purity. **C,** Genes differentially upregulated in the low purity group were also enriched in immune relevant processes. **D,** GSEA indicated a significantly enhanced immune phenotype in cases with low purity. **E,** Associations between glioma purity and immune cell enrichment. **F,** Two clusters of immune cells could be summarized according to their mutual relationship. **G** and **H,** Immunohistochemical analysis verified that macrophages, microglia, and neutrophils were highly enriched in low purity cases. **I–K,** Survival curves indicated that the enrichment of macrophages and neutrophils, but not microglia, conferred poor prognosis.

Published OnlineFirst July 28, 2017; DOI: 10.1158/1078-0432.CCR-16-2598

significantly effective even among gliomas with high purity. Tight associations between glioma purity and genomic indicators implied that the prognostic and predictive value of genomic indicators may be partially derived from their roles in monitoring a balance between tumor and nontumor cells (36). These results highlight the pivotal role of nontumor cells in determining prognosis and question the use of traditional indicators for clinical prediction, especially in individual cases. Here, we have developed a prognostic nomogram comprehensively taking glioma purity and other robust indicators into consideration, which showed superior validity in predicting survival time. Therefore, integrating glioma purity into a prognostic system would be helpful for precise prediction.

Stromal and immune cells constitute the major nontumor fraction within a glioma microenvironment. Moreover, there was a tight association between stromal and immune scores. Distinct local immune status was the primary differential phenotype that resulted from various glioma purities, which was significantly enhanced in cases with low purity. This verifies our previous report, which found that an intensive local immune response is unfavorable for glioma prognosis (37). Importantly, not all immune cells were enriched in tissues with low glioma purity, summarizing two subgroups of immune cells based on their relationship with glioma purity. This highlights the inability of antitumor immune cells in infiltrating into the established protective shield around the glioma cell. These antitumor cells could be represented by CD8 T cells and NK cells, whose enrichment could significantly prolong patients' survival (38, 39).

We should also note the ability of glioma cells in selectively recruiting immune cells to establish a proper microenvironment. We found that macrophages, microglia, and neutrophils were enriched in low purity cases, which could be verified using histologic methods. These cells were of myeloid lineage and associated with cellular immunosuppression in glioma (40). In particular, glioma-associated macrophages and microglia have been reported to form as many as 30% to 50% of the cells in gliomas (5). Different polarization statuses of macrophages and microglia have been defined based on stimulation *in vitro*, including the classical M1 phenotype and alternative M2 phenotype. Their enrichment generally contributes to the glioma growth, invasion, and increasing histopathologic grade (41). Previous studies deemed macrophage and microglia as unfavorable indicators for prognosis (41–43). Whereas, only macrophage was identified with prognostic significance in the present study. Unlike previous results which were mainly derived from analysis on a single marker, we evaluated the enrichment of macrophage and microglia by conducting a GSVA algorithm that was based on the expression profile of a characteristic gene set and generated a signature from a more comprehensive perspective. Although there are abundant studies that focus on the role of macrophages and microglia, further analysis is still needed to confirm our results and explore the different roles of polarization in glioma.

However, low purity glioma contains abundant neutrophil infiltration, which is positively associated with grade progression, shorter survival, and treatment resistance (44–46). A previous study reported complex interaction among neutrophils, macrophages, and microglia. This interaction is critical in maintaining glioma's local immunosuppressive phenotype (47). Neutrophils also inhibit the cytolytic activity of NK cells and CD8 T cells (45). Therefore, blocking neutrophil infiltration could be suggested for combined treatment strategy. Considering the tight association between the neutrophil-to-lymphocyte ratio in peripheral blood and local neutrophil infiltration, the neutrophil-to-lymphocyte ratio may be an invasive indicator for evaluating the treatment response (45).

Specific genomic alterations have been established as early event initiating gliomagenesis (32). Here, we observed distinct genomic patterns attributing to various glioma purities. Despite there being doubt that low purity may reduce the sensitivity of somatic mutation and CNA testing (48), we still detected negative correlation between glioma purity and events of genomic alteration, indicating an instable genomic status in low purity cases. Therefore, genomic alterations and heterogeneity may have substantial roles in editing the glioma microenvironment. The low purity induced an intensive immune phenotype that could further aggravate the genomic instability (49), thus creating a positive feedback that exacerbates the poor prognosis and treatment resistance (50).

The main advantage of our research was the use of large sample-sized glioma cohorts and systematic analysis in multidimensional conditions. Our findings highlight the important role of tumor purity and local immune cells in glioma biology and clinical management. However, we still need to clarify the extent and type of immune responses that can promote glioma progression. It would be interesting to depict cellular components within a microenvironment, interpret their clinical implications, and explore the immunoregulatory role of glioma cells.

Taken together, glioma purity exerted a considerable effect on clinical, genomic, and biological conditions. Assessing the proportion of different cell types may help in elucidating the complex role of glioma microenvironment and provide new insights into its clinical management. An ideal classification system should focus not only on the properties of tumor cells but also on nontumor cells.

Disclosure of Potential Conflicts of Interest

No potential conflicts of interest were disclosed.

Authors' Contributions

Conception and design: W. Cheng, G. Li, S. Han, T. Jiang, A. Wu
Development of methodology: C. Zhang, W. Cheng, A. Wu
Acquisition of data (provided animals, acquired and managed patients, provided facilities, etc.): C. Zhang, W. Cheng, X. Ren, X. Liu, G. Li, T. Jiang, A. Wu
Analysis and interpretation of data (e.g., statistical analysis, biostatistics, computational analysis): C. Zhang, W. Cheng, X. Ren, Z. Wang, G. Li, S. Han, A. Wu
Writing, review, and/or revision of the manuscript: C. Zhang, W. Cheng, G. Li, T. Jiang, A. Wu
Administrative, technical, or material support (i.e., reporting or organizing data, constructing databases): C. Zhang, W. Cheng, X. Ren, G. Li, T. Jiang
Study supervision: T. Jiang, A. Wu

Acknowledgments

The authors conducting this work represent the Chinese Glioma Cooperative Group (CGCG). We thank Lin Fu and Qingchang Li at the Department of Pathology, the First Affiliated Hospital of China Medical University, for assistance in morphology analysis.

Grant Support

This work was supported by grants from the National Natural Science Foundation of China [Grant Numbers: 81172409 (A. Wu), 81472360 (A. Wu), and 81402045 (S. Han)], the Science and Technology Department of Liaoning Province [Grant Number: 2011225034 (A. Wu)], the National Key Research and

Development Plan [Grant Number: 2016YFC0902500 (T. Jiang)], and the Capital Medical Development Research Fund [Grant Number: 2016-1-1072 (T. Jiang)].

The costs of publication of this article were defrayed in part by the payment of page charges. This article must therefore be hereby marked *advertisement* in accordance with 18 U.S.C. Section 1734 solely to indicate this fact.

Received October 16, 2016; revised April 26, 2017; accepted July 20, 2017; published OnlineFirst July 28, 2017.

References

1. Louis DN, Perry A, Reifenberger G, von Deimling A, Figarella-Branger D, Cavenee WK, et al. The 2016 World Health Organization classification of tumors of the central nervous system: a summary. Acta Neuropathol 2016;131:803–20.
2. Dunn GP, Rinne ML, Wykosky J, Genovese G, Quayle SN, Dunn IF, et al. Emerging insights into the molecular and cellular basis of glioblastoma. Genes Dev 2012;26:756–84.
3. Westphal M, Lamszus K. The neurobiology of gliomas: from cell biology to the development of therapeutic approaches. Nat Rev Neurosci 2011; 12:495–508.
4. Golebiewska A, Bougnaud S, Stieber D, Brons NH, Vallar L, Hertel F, et al. Side population in human glioblastoma is non-tumorigenic and characterizes brain endothelial cells. Brain 2013;136:1462–75.
5. Hambardzumyan D, Gutmann DH, Kettenmann H. The role of microglia and macrophages in glioma maintenance and progression. Nat Neurosci 2016;19:20–7.
6. Hossain A, Gumin J, Gao F, Figueroa J, Shinojima N, Takezaki T, et al. Mesenchymal stem cells isolated from human gliomas increase proliferation and maintain stemness of glioma stem cells through the IL-6/gp130/STAT3 pathway. Stem Cells 2015;33:2400–15.
7. Huang Y, Hoffman C, Rajappa P, Kim JH, Hu W, Huse J, et al. Oligodendrocyte progenitor cells promote neovascularization in glioma by disrupting the blood-brain barrier. Cancer Res 2014;74:1011–21.
8. Vartanian A, Singh SK, Agnihotri S, Jalali S, Burrell K, Aldape KD, et al. GBM's multifaceted landscape: highlighting regional and microenvironmental heterogeneity. Neuro Oncol 2014;16:1167–75.
9. Rape A, Ananthanarayanan B, Kumar S. Engineering strategies to mimic the glioblastoma microenvironment. Adv Drug Deliv Rev 2014;79–80:172–83.
10. Dunn GP, Bruce AT, Ikeda H, Old LJ, Schreiber RD. Cancer immunoediting: from immunosurveillance to tumor escape. Nat immunol 2002;3: 991–8.
11. Silver DJ, Sinyuk M, Vogelbaum MA, Ahluwalia MS, Lathia JD. The intersection of cancer, cancer stem cells, and the immune system: therapeutic opportunities. Neuro Oncol 2016;18:153–9.
12. Kioi M, Vogel H, Schultz G, Hoffman RM, Harsh GR, Brown JM. Inhibition of vasculogenesis, but not angiogenesis, prevents the recurrence of glioblastoma after irradiation in mice. J Clin Invest 2010;120:694–705.
13. Yoshihara K, Shahmoradgoli M, Martinez E, Vegesna R, Kim H, Torres-Garcia W, et al. Inferring tumour purity and stromal and immune cell admixture from expression data. Nat Commun 2013;4:2612.
14. Bao ZS, Chen HM, Yang MY, Zhang CB, Yu K, Ye WL, et al. RNA-seq of 272 gliomas revealed a novel, recurrent PTPRZ1-MET fusion transcript in secondary glioblastomas. Genome Res 2014;24:1765–73.
15. Mortazavi A, Williams BA, McCue K, Schaeffer L, Wold B. Mapping and quantifying mammalian transcriptomes by RNA-Seq. Nat Methods 2008;5:621–8.
16. Yan W, Zhang W, You G, Bao Z, Wang Y, Liu Y, et al. Correlation of IDH1 mutation with clinicopathologic factors and prognosis in primary glioblastoma: a report of 118 patients from China. PloS One 2012;7: e30339.
17. Yang P, Cai J, Yan W, Zhang W, Wang Y, Chen B, et al. Classification based on mutations of TERT promoter and IDH characterizes subtypes in grade II/III gliomas. Neuro Oncol 2016;18:1099–108.
18. Cheng W, Li M, Jiang Y, Zhang C, Cai J, Wang K, et al. Association between small heat shock protein B11 and the prognostic value of MGMT promoter methylation in patients with high-grade glioma. J Neurosurg 2016;125: 7–16.
19. Verhaak RG, Hoadley KA, Purdom E, Wang V, Qi Y, Wilkerson MD, et al. Integrated genomic analysis identifies clinically relevant subtypes of glioblastoma characterized by abnormalities in PDGFRA, IDH1, EGFR, and NF1. Cancer Cell 2010;17:98–110.
20. Sun Y, Zhang W, Chen D, Lv Y, Zheng J, Lilljebjorn H, et al. A glioma classification scheme based on coexpression modules of EGFR and PDGFRA. Proc Natl Acad Sci U S A 2014;111:3538–43.
21. Ogata H, Goto S, Sato K, Fujibuchi W, Bono H, Kanehisa M. KEGG: Kyoto Encyclopedia of Genes and Genomes. Nucleic Acids Res 1999;27:29–34.
22. Huang da W, Sherman BT, Lempicki RA. Systematic and integrative analysis of large gene lists using DAVID bioinformatics resources. Nature protocols 2009;4:44–57.
23. Subramanian A, Tamayo P, Mootha VK, Mukherjee S, Ebert BL, Gillette MA, et al. Gene set enrichment analysis: a knowledge-based approach for interpreting genome-wide expression profiles. Proc Natl Acad Sci U S A 2005;102:15545–50.
24. Hanzelmann S, Castelo R, Guinney J. GSVA: gene set variation analysis for microarray and RNA-seq data. BMC Bioinformatics 2013;14:7.
25. Bindea G, Mlecnik B, Tosolini M, Kirilovsky A, Waldner M, Obenauf AC, et al. Spatiotemporal dynamics of intratumoral immune cells reveal the immune landscape in human cancer. Immunity 2013;39:782–95.
26. Butovsky O, Jedrychowski MP, Moore CS, Cialic R, Lanser AJ, Gabriely G, et al. Identification of a unique TGF-beta-dependent molecular and functional signature in microglia. Nat Neurosci 2014;17:131–43.
27. Wang Y, Li J, Xia Y, Gong R, Wang K, Yan Z, et al. Prognostic nomogram for intrahepatic cholangiocarcinoma after partial hepatectomy. J Clin Oncol 2013;31:1188–95.
28. Aran D, Sirota M, Butte AJ. Systematic pan-cancer analysis of tumour purity. Nat Commun 2015;6:8971.
29. Carter SL, Cibulskis K, Helman E, McKenna A, Shen H, Zack T, et al. Absolute quantification of somatic DNA alterations in human cancer. Nat Biotechnol 2012;30:413–21.
30. Eckel-Passow JE, Lachance DH, Molinaro AM, Walsh KM, Decker PA, Sicotte H, et al. Glioma groups based on 1p/19q, IDH, and TERT promoter mutations in tumors. N Engl J Med 2015;372:2499–508.
31. Cancer Genome Atlas Research N, Brat DJ, Verhaak RG, Aldape KD, Yung WK, Salama SR, et al. Comprehensive, integrative genomic analysis of diffuse lower-grade gliomas. N Engl J Med 2015;372:2481–98.
32. Suzuki H, Aoki K, Chiba K, Sato Y, Shiozawa Y, Shiraishi Y, et al. Mutational landscape and clonal architecture in grade II and III gliomas. Nat Genet 2015;47:458–68.
33. Cohen DA, Dabbs DJ, Cooper KL, Amin M, Jones TE, Jones MW, et al. Interobserver agreement among pathologists for semiquantitative hormone receptor scoring in breast carcinoma. Am J Clin Pathol 2012; 138:796–802.
34. Zhu W, Kuziora M, Creasy T, Lai Z, Morehouse C, Guo X, et al. BubbleTree: an intuitive visualization to elucidate tumoral aneuploidy and clonality using next generation sequencing data. Nucleic Acids Res 2016;44:e38.
35. Zheng X, Zhao Q, Wu HJ, Li W, Wang H, Meyer CA, et al. MethylPurify: tumor purity deconvolution and differential methylation detection from single tumor DNA methylomes. Genome Biol 2014;15:419.
36. Ying H, Elpek KG, Vinjamoori A, Zimmerman SM, Chu GC, Yan H, et al. PTEN is a major tumor suppressor in pancreatic ductal adenocarcinoma and regulates an NF-kappaB-cytokine network. Cancer Discov 2011; 1:158–69.
37. Cheng W, Ren X, Zhang C, Cai J, Liu Y, Han S, et al. Bioinformatic profiling identifies an immune-related risk signature for glioblastoma. Neurology 2016;86:2226–34.
38. Ogbomo H, Cinatl J Jr., Mody CH, Forsyth PA. Immunotherapy in gliomas: limitations and potential of natural killer (NK) cell therapy. Trends Mol Med 2011;17:433–41.
39. Han S, Zhang C, Li Q, Dong J, Liu Y, Huang Y, et al. Tumour-infiltrating CD4(+) and CD8(+) lymphocytes as predictors of clinical outcome in glioma. Br J Cancer 2014;110:2560–8.
40. Gabrilovich DI, Nagaraj S. Myeloid-derived suppressor cells as regulators of the immune system. Nat Rev Immunol 2009;9:162–74.

41. Hambardzumyan D, Gutmann DH, Kettenmann H. The role of microglia and macrophages in glioma maintenance and progression. Nat Neurosci 2015;19:20–7.
42. Komohara Y, Ohnishi K, Kuratsu J, Takeya M. Possible involvement of the M2 anti-inflammatory macrophage phenotype in growth of human gliomas. J Pathol 2008;216:15–24.
43. Pong WW, Walker J, Wylie T, Magrini V, Luo J, Emnett RJ, et al. F11R is a novel monocyte prognostic biomarker for malignant glioma. PloS one 2013;8:e77571.
44. Fossati G, Ricevuti G, Edwards SW, Walker C, Dalton A, Rossi ML. Neutrophil infiltration into human gliomas. Acta Neuropathol 1999;98:349–54.
45. Han S, Liu Y, Li Q, Li Z, Hou H, Wu A. Pre-treatment neutrophil-to-lymphocyte ratio is associated with neutrophil and T-cell infiltration and predicts clinical outcome in patients with glioblastoma. BMC Cancer 2015;15:617.
46. Liang J, Piao Y, Holmes L, Fuller GN, Henry V, Tiao N, et al. Neutrophils promote the malignant glioma phenotype through S100A4. Clin Cancer Res 2014;20:187–98.
47. Zhou SL, Zhou ZJ, Hu ZQ, Huang XW, Wang Z, Chen EB, et al. Tumor-associated neutrophils recruit macrophages and T-regulatory cells to promote progression of hepatocellular carcinoma and resistance to sorafenib. Gastroenterology 2016;150:1646–58 e17.
48. Ding L, Getz G, Wheeler DA, Mardis ER, McLellan MD, Cibulskis K, et al. Somatic mutations affect key pathways in lung adenocarcinoma. Nature 2008;455:1069–75.
49. Grivennikov SI, Greten FR, Karin M. Immunity, inflammation, and cancer. Cell 2010;140:883–99.
50. Cheng W, Li M, Cai J, Wang K, Zhang C, Bao Z, et al. HDAC4, a prognostic and chromosomal instability marker, refines the predictive value of MGMT promoter methylation. J Neuro Oncol 2015;122:303–12.

Published OnlineFirst July 28, 2017; DOI: 10.1158/1078-0432.CCR-16-2598

Clinical Cancer Research

Tumor Purity as an Underlying Key Factor in Glioma

Chuanbao Zhang, Wen Cheng, Xiufang Ren, et al.

Clin Cancer Res 2017;23:6279-6291. Published OnlineFirst July 28, 2017.